EDWARDS AQUIFER PARAMETER ESTIMATION PROJECT: FINAL REPORT

Prepared for

Edwards Aquifer Authority

Center for Nuclear Waste Regulatory Analyses
San Antonio, Texas

SwRI Logo

EDWARDS AQUIFER PARAMETER ESTIMATION PROJECT: FINAL REPORT

Prepared by

Scott Painter
Center for Nuclear Waste Regulatory Analyses
San Antonio, Texas

Yefang Jiang
Allan Woodbury
University of Manitoba
Winnipeg, Manitoba, Canada

April 2002

ABSTRACT

This work supports ongoing efforts by the Edwards Aquifer Authority to develop a groundwater management model of the San Antonio segment of the Edwards Aquifer. Values of hydraulic conductivity, a key parameter controlling groundwater flow, are assigned to the model grid developed by the U.S. Geological Survey (USGS). The approach used, a combination of spatial statistical methods and advanced techniques for automatic model calibration, incorporates existing data of various types and avoids manual adjustment of the hydraulic conductivity distribution.

Hydraulic conductivity in heterogeneous aquifers depends on the spatial scale of the measurement. Existing hydraulic conductivity measurements in the Edwards Aquifer are mostly from single-well drawdown tests and are appropriate for the spatial scale of a few meters. These need to be modified or upscaled before being applied to the 402 m × 402 m computational cells intended for the management model. An approach based on nonparametric geostatistics, stochastic simulation, and numerical flow simulation was used to upscale and interpolate to the groundwater management model grid. This formed Revision 1 of the hydraulic conductivity model.

Revision 1 of the hydraulic conductivity honored existing hydraulic conductivity measurements, but does not honor measurements of hydraulic heads. Hydraulic heads carry significant information about the underlying hydraulic conductivity distribution, but using hydraulic heads to infer hydraulic conductivity has no unique result and is poorly suited for numerical calculation. A recent approach for automatic model calibration based on Bayesian statistics was used to generate the final hydraulic conductivity model (Revision 3), which matches hydraulic head measurements. This approach uses statistical methods to pick from the universe of potential hydraulic conductivity models the one that minimizes deviation from a preconceived or prior model. This step required the construction of a groundwater flow model incorporating boundary conditions, aquifer thickness, pumpage, and recharge rates provided by USGS. Thus, it merges data of various types in a way that also honors the physics of groundwater flow.

A fully calibrated model was not one of the original goals of this project. Nevertheless, a hydraulic conductivity model calibrated to steady-state hydraulic head measurements and partially calibrated to steady-state spring discharges was achieved. With each new revision of the hydraulic conductivity model, the match between the calculated and observed hydraulic heads and spring flows improved, thereby demonstrating the utility of the approach. The final hydraulic conductivity model provides a starting point for conventional manual model calibration. With some modest refinements, the approach developed and applied here could also be used in fully automatic model calibrations.

3/37

CONTENTS

4/3.7

FIGURES

5/37

TABLES

6/37

ACKNOWLEDGMENTS

This report was prepared to document work performed by the Center for Nuclear Waste Regulatory Analyses (CNWRA) for the Edwards Aquifer Authority (EAA). The report is an independent product of the CNWRA and does not necessarily reflect the views or regulatory position of the EAA.

The authors are grateful to Paulette Houston for help formatting this report. We also thank Ron Green and Budhi Sagar for careful review of the manuscript.

QUALITY OF DATA, ANALYSES, AND CODE DEVELOPMENT

DATA: No new data were generated in this work.

ANALYSES AND CODES: The computer codes used in this analysis are single-use codes and are not controlled under the CNWRA software control procedure TOP-018. The computer codes and associated input and output files are included in the CNWRA quality assurance record through CNWRA Scientific Notebook SN469E.

7/37

1 INTRODUCTION AND BACKGROUND

The U.S. Geological Survey (USGS) and the Texas Bureau of Economic Geology (BEG) are currently developing a groundwater management model of the San Antonio segment of the Edwards Aquifer. After calibrating to historical data on hydraulic heads and spring discharge rates, the two-dimensional model will be used to assess various groundwater management scenarios for the Edwards Aquifer. To support the USGS and BEG effort, the Center for Nuclear Waste Regulatory Analyses (CNWRA), a division of the Southwest Research Institute™, developed an improved model for hydraulic conductivity in the Edwards Aquifer. This report describes the results of this Edwards Aquifer Parameter Estimation Project.

The broad objective of the Parameter Estimation Project is to provide improved representations of the areal distribution of vertically averaged hydraulic conductivity across the San Antonio region of the Edwards Aquifer using the best available quantitative techniques. The specific objectives are (i) to interpolate existing sparse measurements of hydraulic conductivity to model grid locations provided by the USGS and (ii) to address the discrepancy in spatial scale between the single-borehole based hydraulic conductivity measurements and the 402 m × 402 m (1/4 mi × 1/4 mi) grid cells. The second issue arises because hydraulic conductivity in a heterogeneous medium is dependent on the scale at which it is defined. Thus, single-borehole based measurements, which investigate the scale of a few meters, need to be modified or "upscaled" before being used in the USGS model. A statistical framework was selected at the beginning of the project to minimize subjective input and thus, maximize defensibility of the model in a legal setting.

Development of the hydraulic conductivity model proceeded in stages. An initial properties model was delivered to the Edwards Aquifer Authority in November 2000. This initial model was intended to be a "placeholder" for use by the USGS in developing and debugging the groundwater management model. The initial model was replaced by Revision 1 in July 2001, which was intended to support steady-state calibration of the management model. Following delivery of Revision 1, it was determined that the quality of the hydraulic conductivity data was insufficient to justify further analyses with this data alone, and it was decided to also incorporate hydraulic head data. Using hydraulic head data to infer hydraulic conductivity is a process known as "inverse modeling" or "parameter estimation by inversion." In general, inversion is difficult because the solution is nonunique and the calculations are subject to numerical instabilities. However, recent years have seen important progress in the technology of inverse modeling, and a suitable approach based on Bayesian statistics was identified. This approach has the important advantage of being able to use directly the existing work on upscaled hydraulic conductivity (Revision 1). Revision 2 of the hydraulic conductivity model, delivered in March 2002, was a preliminary application of the Bayesian technique. Revision 3 of the hydraulic conductivity model, which is included with this report, represents a further refinement of the approach.

In the remainder of this report, the analyses leading to Revision 3 of the hydraulic conductivity model are described, the performance of the models are assessed using groundwater flow simulations, and some suggested approaches for future refinements of the model are provided. Revision 2 is not described because it is completely replaced by the final property model. The geostatistical analysis used to generate Revision 1 is included because it forms the starting point for Revision 3.

8/37

2 HYDRAULIC CONDUCTIVITY DATA

The starting point in the analysis is the transmissivity/hydraulic conductivity dataset provided by BEG (Mace, 2000; Mace and Hovorka, 2000; Hovorka, et al., 1998). Although a few data are from traditional aquifer tests, most of these data are from single borehole tests and are thus appropriate for the local scale (a few meters). Transmissivity estimates for the single-well tests were obtained from measured specific capacity using a relationship between transmissivity and specific capacity that was determined empirically for the Edwards Aquifer (Mace, 2000). Vertically averaged hydraulic conductivity K was then obtained from transmissivity by dividing by the screened interval of the well. The only manipulation of the data performed for the present study was to geometrically average values when multiple values (representing different tests) exist for the same well. After this averaging, the dataset contains 653 values of hydraulic conductivity in the confined zone and 108 values in the unconfined zone. Data locations are shown in Figure 2-1. The color scale is logarithmic in K with warm colors representing large values.

2.1 Univariate Statistics

Univariate statistical distributions of hydraulic conductivity data are shown in Figure 2-2 for the confined and unconfined sections of the Edwards Aquifer. Both distributions are reasonably well approximated as lognormal, although the hydraulic conductivity distribution for the confined section does have a lower tail that is enhanced relative to the lognormal distribution. The mean and variance for the confined and unconfined sections are significantly different, which is the main motivation for treating them as separate populations. The geometric mean is 5.7 m/d (18.8 ft/d) for the confined section compared to 0.4 m/d (1.3 ft/d) for the unconfined zone. The variance in log-K is 6.4 and 9.7 for the confined and unconfined sections. Since it is vertically averaged hydraulic conductivity that is analyzed and not transmissivity, the differences are not due to differences in aquifer thickness between the confined and unconfined zones. The cause of the smaller hydraulic conductivity in the unconfined zone is not clear, but it is noted that lower values of hydraulic conductivity in the unconfined region would result if the most permeable subunits of the Edwards group were located near the top of the formation.

2.2 Data Limitations and Potential Effects on the Analyses

The data from the single well tests have three principal limitations:

1. The empirical correlation between transmissivity and specific capacity is strong but imperfect; and for a given specific capacity value there may be as much as an order-of-magnitude spread in the corresponding transmissivity values. Thus, the data forming the starting point of the study have significant uncertainty. This uncertainty has two consequences: it enhances the spread in the univariate distribution as compared with the true hydraulic conductivity, and tends to mask spatial correlation. Given that Mace and Hovorka (2000) found that transmissivity values as inferred from drawdown and recovery data range over five orders of magnitude, the additional spreading introduced by an order-of-magnitude spread in the specific capacity versus transmissivity relationship is relatively unimportant. The second effect, the masking of spatial correlation, is likely to be more important. This effect is manifest as an increased

9/3-7

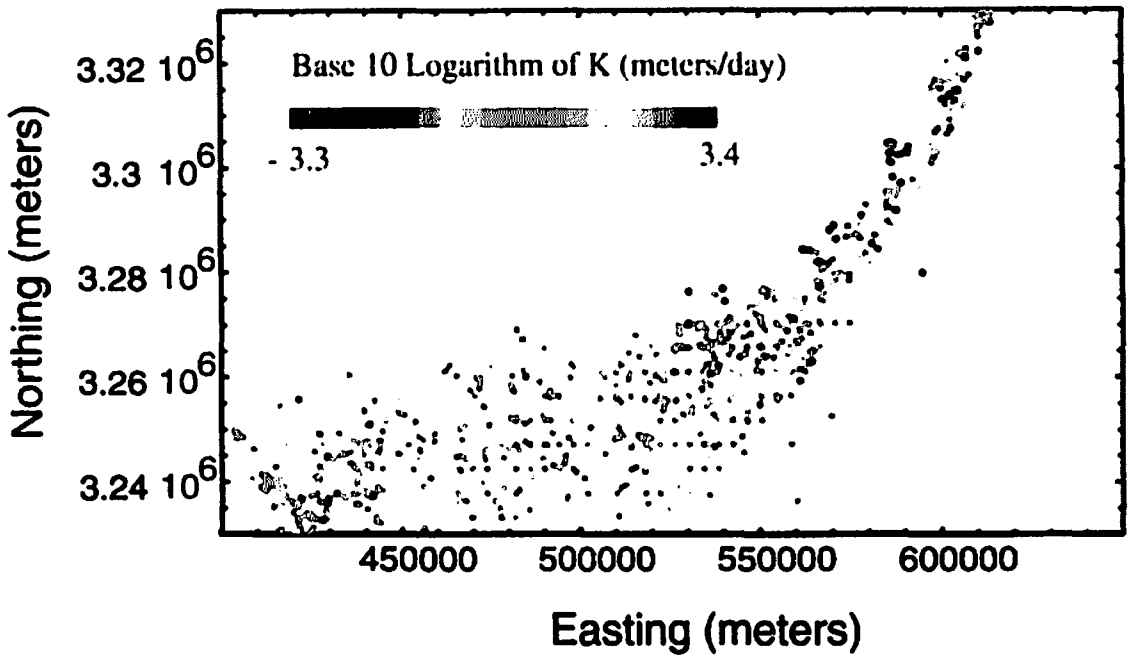

Figure 2-1. Well locations used to form the basis of the geostatistical interpolation. Points are colored coded according to hydraulic conductivity on a logarithmic scale. Warm colors represent high values.

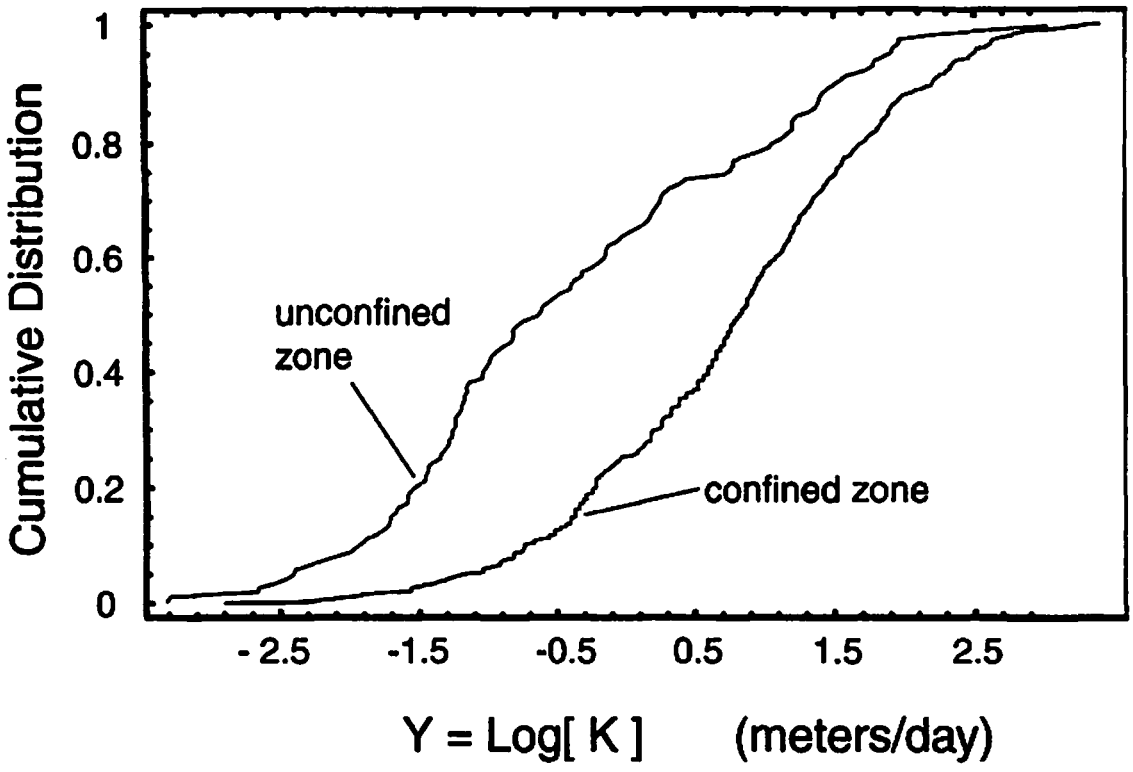

Figure 2-2. Distribution of hydraulic conductivity K on base-10 logarithmic scale for confined and unconfined zones of the Edward Aquifer

11/37

"nugget effect" in the spatial correlation, with the result being to increasing uncertainty in interpolations at points near to the actual measurements.

2. Nearly 15 percent of the single well tests have drawdown that is below the limit of detection and recorded as zero. These tests clearly represent large K values and to discard them would introduce significant bias in the result. In the Mace dataset, these single-well tests have been assigned a drawdown of 0.3 m (1 ft), which is thought to be near the limit of detection for drawdown (Mace and Hovorka, 2000). Hydraulic conductivities based on these wells represent a lower bound on their true hydraulic conductivity. Thus, the data are biased toward low values. Figure 2-3 compares the hydraulic conductivity distributions for the confined zone with and without the zero-drawdown tests.

3. The location data are imprecise for some of the hydraulic conductivity data. This imprecision can be seen by visual examination of the data locations in Figure 2-1. Note that some of the measurements are arranged into horizontal lines. This is thought to be caused by imprecise recording of well location in driller's records. The net effect of this location imprecision is to mask spatial correlation similar to that described in the principal limitation 1.

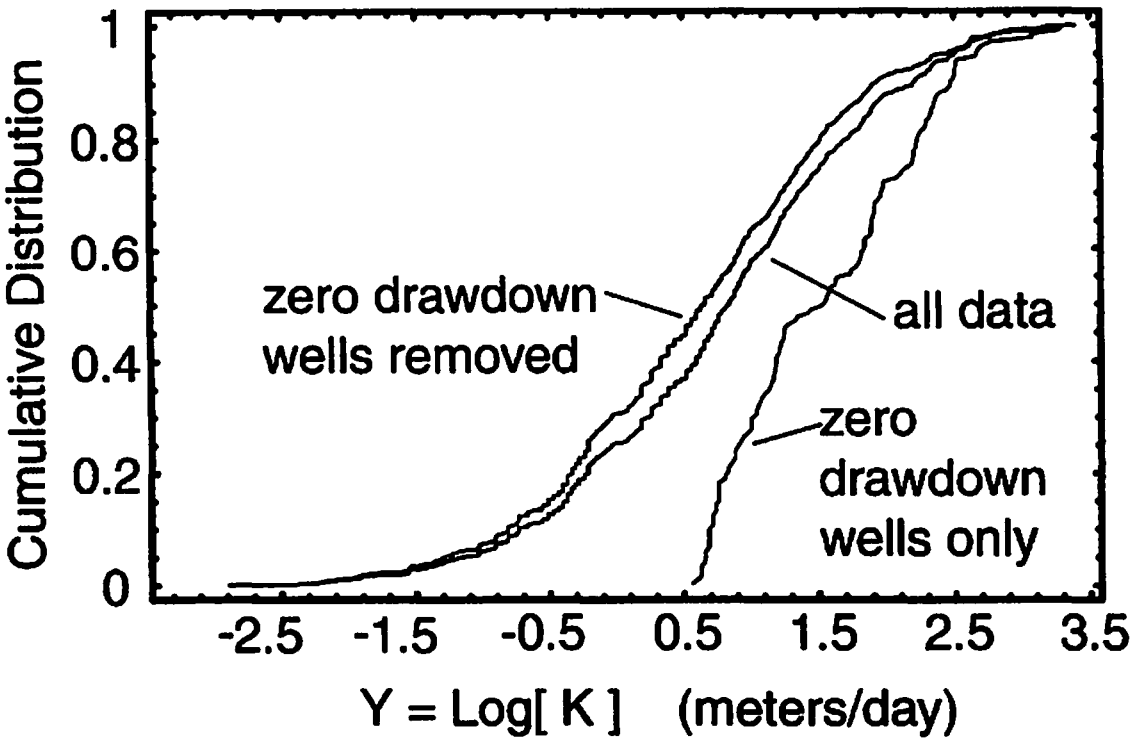

Figure 2-3. Distribution of hydraulic conductivity K on base-10 logarithmic scale for the confined zone with and without the zero drawdown wells. Hydraulic conductivity for zero-drawdown wells was calculated by assuming a drawdown of 0.3 m.

3 REVISION 1: UPSCALING AND INTERPOLATING THE HYDRAULIC CONDUCTIVITY DATABASE

To produce Revision 1 of the hydraulic conductivity model, a simulation approach was developed that addresses data interpolation and the issue of scale consistency in hydraulic conductivity. Data interpolation is necessary because the grid blocks used in the groundwater management model do not necessarily correspond to well locations where measurements of hydraulic conductivity are available. Scale consistency is an issue because hydraulic conductivity in heterogeneous formations is dependent on the scale over which it is defined. If local-scale (a few meters) hydraulic conductivity derived from well tests is applied unaltered to the 402 m (l/4 mi) grid blocks that comprise the USGS management model, it will introduce systematic bias towards lower conductivity values. In constructing a hydraulic conductivity model for the Edwards Aquifer, a geostatistical approach was combined with numerical simulations to address the scale dependencies and thus avoid this systematic bias.

The geostatistical approach is outlined in Figure 3-1. As described in greater detail below, the procedure involves geostatistical analysis of the local scale hydraulic conductivity K, unconditional stochastic simulation of K, numerical flow modeling to generate grid block scale hydraulic conductivity $\overline{K}$, geostatistical analysis of the $\overline{K}$, and cokriging of $\overline{K}$ with the local-scale K data.

3.1 Geostatistical Analysis

The first step in the process is geostatistical analysis of the local-scale conductivity K to establish models for the univariate distribution and the spatial correlation. The confined and unconfined sections of the aquifer were treated as separate populations, and a more detailed geostatistical analysis was undertaken for the confined region to better model spatial correlation in the extreme values of K.

The next step is to establish a model for the two-point spatial correlation. There are several methods for doing this, each with its advantages and disadvantages in a given situation (e.g., Journel and Huijbregts, 1978; Deutsch and Journel, 1998). The most familiar approach is the sample semi-variogram, which is the sample semi-variance as a function of lag (separation) distance. The sample semi-variogram of some random field Z(**u**) is computed as

$$\hat{\gamma}(\mathbf{h}) = \frac{1}{2N(\mathbf{h})}\sum_{\alpha=1}^{N(\mathbf{h})}\left[z(\mathbf{u}_\alpha) - z(\mathbf{u}_\alpha + \mathbf{h})\right]^2 \qquad (3\text{-}1)$$

where **h** is a lag (separation) vector, $z(\mathbf{u}_\alpha)$ is the datum value at location $\mathbf{u}_\alpha$, and N(**h**) is the number of pairs of data separated by the vector distance **h**. The semi-variogram has a simple relationship to the two-point spatial covariance, $\langle Z(\mathbf{u})Z(\mathbf{u}+\mathbf{h})\rangle - \langle Z(\mathbf{u})\rangle\langle Z(\mathbf{u}+\mathbf{h})\rangle$ where angle brackets denote statistical expectation, but is more robust against regional trends in the data.

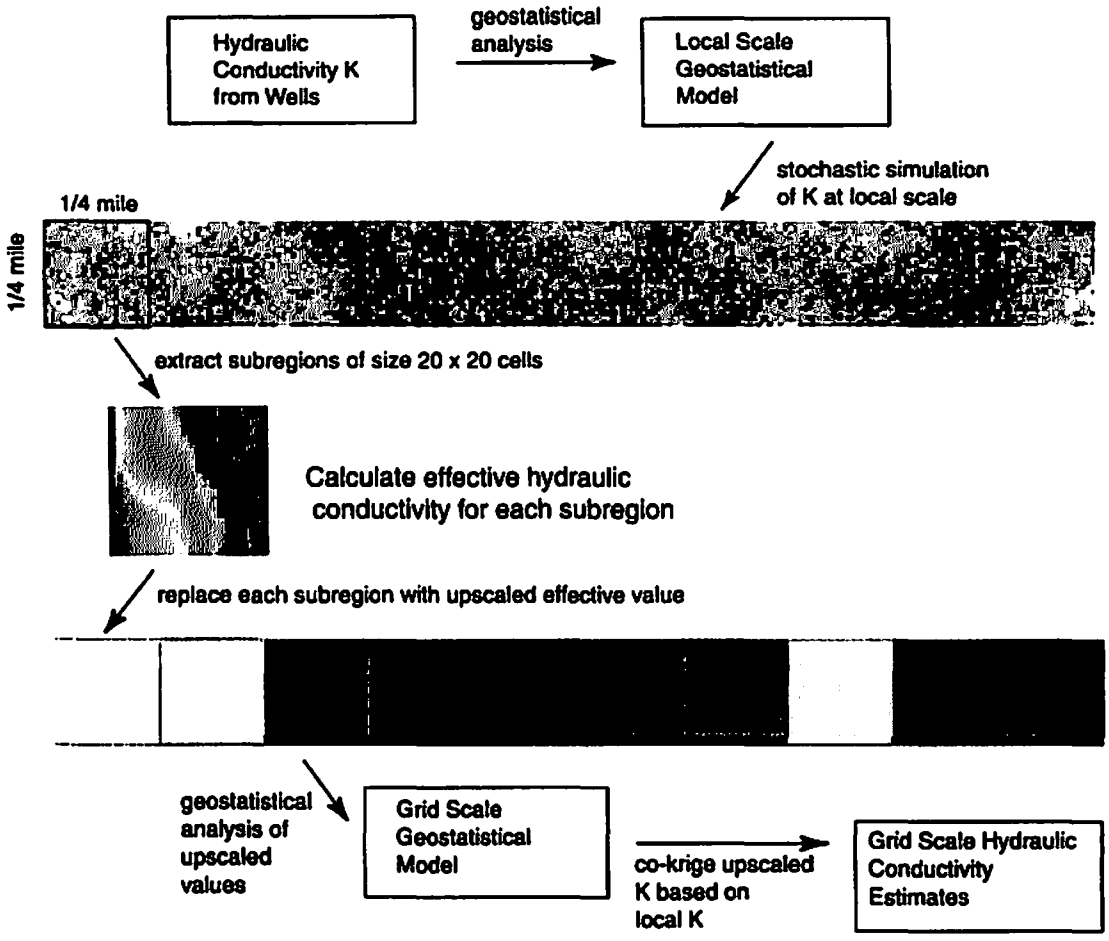

Figure 3-1. Outline of geostatistical procedure used to produce a grid-scale model of hydraulic properties considering the differing scales of support for the measurements and model grids

An alternative approach is to calculate the sample nonergodic covariance

$$\hat{C}(\mathbf{h}) = \frac{1}{N(\mathbf{h})} \sum_{\alpha=1}^{N(\mathbf{h})} z(\mathbf{u}_\alpha) z(\mathbf{u}_\alpha + \mathbf{h}) - \hat{m}_\mathbf{h}^2 \tag{3-2}$$

or the closely related nonergodic correlogram

$$\hat{\rho}(\mathbf{h}) = \frac{\hat{C}(\mathbf{h})}{\hat{\sigma}_\mathbf{h}^2} \tag{3-3}$$

Here $\hat{m}_\mathbf{h}$ and $\hat{\sigma}_\mathbf{h}^2$ are the sample mean and sample variance of the N(h) data pairs, which need not be the same as the mean and variance of the entire population. The correlogram ranges between -1 and 1 with the value 1 corresponding to perfect correlation; the value zero corresponds to the uncorrelated situation.

The semi-variogram is the most widely used measure of spatial correlation. However, it is particularly sensitive to two statistical features that often occur in combination in hydrological data: heteroscedasticity and clustering of extreme values. The term heteroscedasticity refers to the situation when the local variability of the data is related to the local mean, or more generally, changes over the study area. When this occurs in combination with clustering of data, spatial correlation as measured by the semi-variogram, is often masked. The nonergodic correlogram is preferred in such situations, as it is known to be robust against these statistical artifacts (Deutsch and Journel, 1998).

It is advantageous to apply these measures of spatial correlation not to the original K data, but to some transforms of K. For example, it is common to calculate the semi-variogram or correlogram for the logarithmic transforms Y = ln(K). Another powerful technique is to apply the semi-variogram or correlogram to indicator transforms. The indicator transform at a given cutoff value is obtained by replacing those values above the cutoff with a 1 and those below with a 0. By repeating this process for several cutoff values and calculating the variogram or correlogram for each, it is possible to develop a nonparametric model for the spatial correlation. Such an indicator model contains much more information than a traditional semi-variogram model, and is preferred if enough data are available. In particular, an indicator model is better in reproducing spatial correlation in the tails of the distribution, which controls upscaling.

Omnidirectional indicator correlograms for the confined region K are shown in Figure 3-2 for five cutoff values corresponding to the 1st, 2nd, 5th, 8th and 9th decile. The fact that these correlograms are nonzero for nonzero lag distances means that significant spatial correlation exists for all cutoff values. For these data, the indicator correlograms for the 1st decile are larger than the corresponding ones for the median or upper cutoffs. This suggests that low values of K are better correlated spatially than the large values. The fact that all of these are significantly less than 1 as lags approach 0 is a manifestation of the nugget effect. A nonzero nugget value means that K measured in two closely spaced wells would be imperfectly correlated due to the effects of very small scale variability or measurement errors.

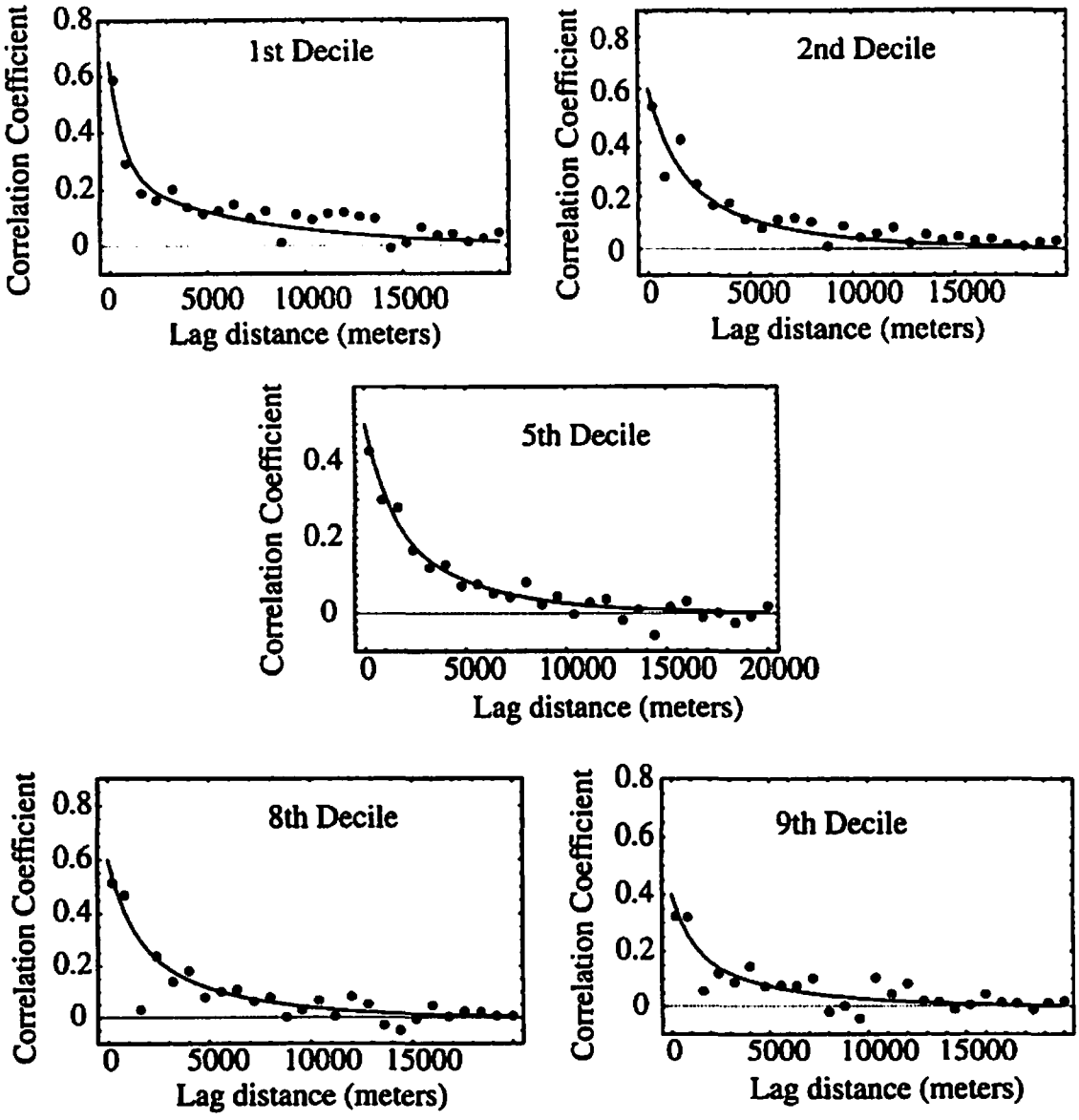

Figure 3-2. Omnidirectional indicator correlograms for hydraulic conductivity in the confined region of the Edwards Aquifer compared with fitted correlation models. A nonzero value for the correlation coefficient at a given lag indicates spatial correlation. Significant spatial correlation is seen for all threshold values, but is stronger for the lowest thresholds. Correlation does not go to 1 at 0 lag because of the nugget effect.

The solid curves in Figure 3-2 are fitted correlogram models. The indicator correlogram for each cutoff is well fitted by a nested exponential model of the form:

$$\rho(h) = p_1 \exp\left(-\frac{h}{\lambda_1}\right) + p_2 \exp\left(-\frac{h}{\lambda_2}\right) \quad (3\text{-}4)$$

where 3 λ_1 and 3 λ_2 are the practical correlation ranges, p_1 and p_2 quantify the relative contributions of the two correlation structures, and $1\text{-}p_1\text{-}p_2$ is the relative nugget value. Values for each cutoff are summarized in Table 3-1. For each cutoff, the two correlation structures contribute roughly equally to the composite correlation structure. The short correlation range is 2.1–3.6 km, depending on the cutoff value, and the long correlation range is 15 km except for the first decile, which has a practical correlation range of 21 km.

The indicator semi-variogram for the 9th decile is shown for comparison purposes in Figure 3-3. The semi-variogram is constant for all lags except for random fluctuations. This suggests no spatial correlation in the upper 10 percent of the K distribution, as opposed to the correlogram in Figure 3-2, which shows significant spatial correlation. Careful review of the data suggests that this apparent discrepancy is caused by m_h and σ^2_h being different for small and large lags, a statistical feature that is known to mask spatial correlation. There are two possible causes for the m_h and σ^2_h being different for small and large lags: heteroscedasticity and sampling bias. Sampling bias is likely in this dataset, as a landowner that drills an unproductive well is likely to try again on the same property. This type of biased sampling may alter the statistics of closely spaced wells compared with the general population. Whatever the cause, the correlogram is robust to this statistical feature and picks up spatial correlation that would have been overlooked using the traditional semi-variogram.

The data from the unconfined zone are too few to support an indicator model and a traditional sample semi-variogram was calculated for Y = ln(K) instead. The results are shown in Figure 3-4. Although noisy due to the small sample size, the semi-variogram does show significant spatial correlation at small lag distances. A spherical semi-variogram model with range of 15 km provides a reasonable fit.

Table 3-1. Parameters in indicator correlation models fitted to confined-zone K data

Threshold	First Correlation Range $3\lambda_1$ (meters)	Second Correlation Range $3\lambda_2$ (meters)	Relative Contribution of First Structure p_1	Relative Contribution of Second Structure p_2
1st decile	2100	21000	0.40	0.22
2nd decile	3600	15000	0.30	0.30
5th decile (median)	3600	15000	0.25	0.25
8th decile	3600	15000	0.30	0.30
9th decile	3000	15000	0.20	0.20

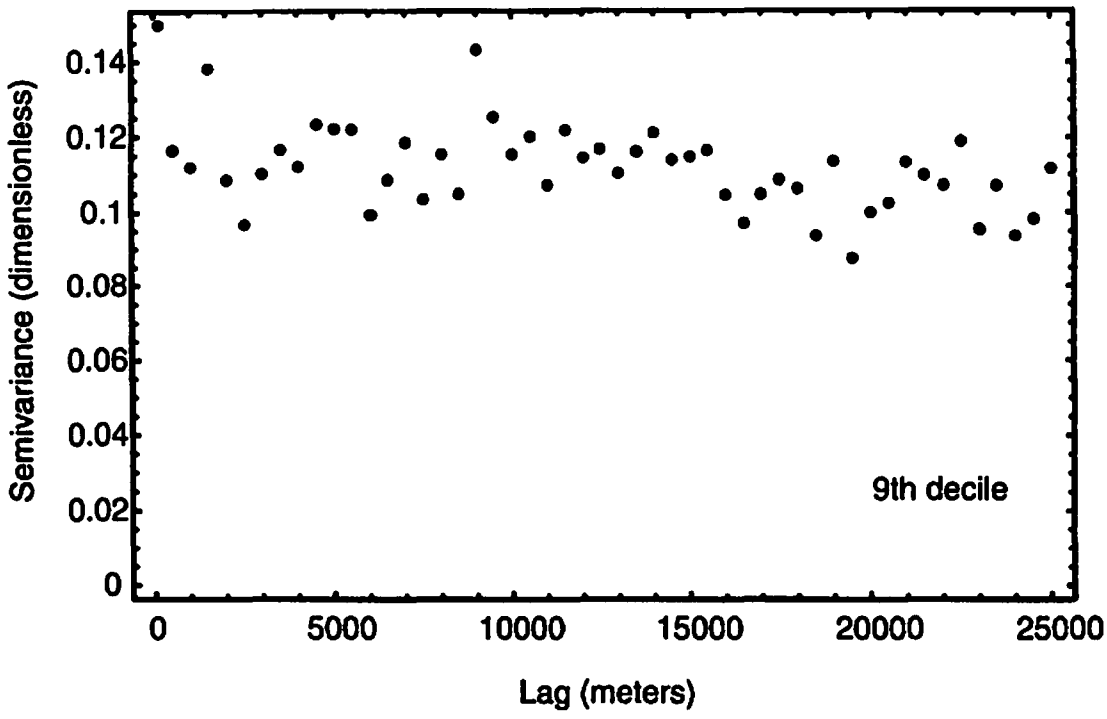

Figure 3-3. Omnidirectional indicator semivariogram for the 9th decile threshold of hydraulic conductivity in the confined zone. No spatial correlation is evident in this plot. Spatial correlation is masked by the statistical artifacts discussed in the text. The correlograms shown in Figure 3-2 are insensitive to this effect.

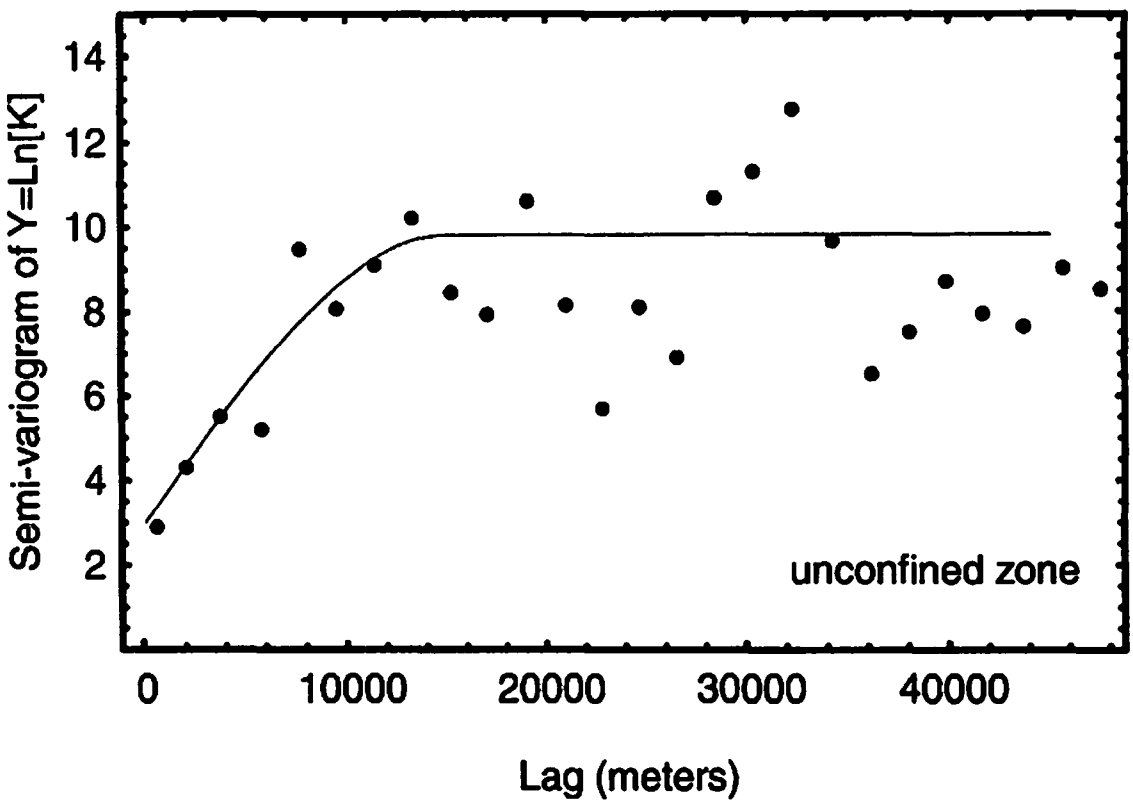

Figure 3-4. Omnidirectional traditional semivariogram for Y=Ln[K] in the unconfined zone. The fitted model semivariogram is a spherical model with range of 15000 m and a relative nugget of 0.3. The traditional semivariogram was used for the unconfined zone because the data from this region are too few to support an indicator model.

3.2 Upscaling from Local to Block Scale

Having established geostatistical models for the confined and unconfined zones which are valid for the scale of the well test data, the next step is to upscale to the 402 m × 402 m (1/4 mi × 1/4 mi) scale of the grid blocks used in the USGS management model. Upscaling in this context means calculating or estimating the univariate distribution of the block-scale hydraulic conductivity $\overline{K}$, and a spatial cross-correlation between $\overline{Y} = \ln \overline{K}$ and Y (the block-to-point cross correlation). Note that the block-to-block correlation is not needed because we have no direct measurements of $\overline{K}$ to match in the interpolation.

For the confined zone, unconditional stochastic simulations of K were obtained using the sequential indicator simulation method as implemented in the SISIM module of the GSLIB (Version 2.1) system (Deutsch and Journel, 1998). This approach does not presume a multigaussian model, and is able to better represent random fields with connected regions of high or low K. Twenty realizations with 20 × 2000 cells in each were generated. Each cell has dimensions of 20 m × 20 m. The geostatistical model fit to the Y data is presumed valid at this scale, because the original well test data support scale (the local scale), from which the geostatistical model was derived, is of comparable size.

To obtain realizations of the $\overline{K}$, each of the 20 × 20 cell subregions (corresponding to the 402 m × 402 m (1/4 mi × 1/4 mi) grid block planned for the USGS management model) were successively removed from the simulated K fields. A head gradient was applied across each subregion in the x-direction with no-flow conditions on the other two sides, and the resulting head calculated using a finite-difference code. Because the fitted geostatistical model is isotropic, numerical flow experiments are required for only one direction. Once the head solution was obtained, the total flux through the subregion was calculated, and then converted to an effective hydraulic conductivity by dividing by the magnitude of the applied gradient. This procedure was repeated for each subregion in each realization. The result is simulated realizations of the $\overline{K}$ field.

These simulated $\overline{K}$ fields were then analyzed statistically. The geometric mean of $\overline{K}$ is increased by 65 percent and the log-variance (variance of $\overline{Y} = \ln \overline{K}$) is decreased by a factor of 32 percent compared with the local scale values. The increase in geometric mean with increasing scale is consistent with previous studies of hydraulic conductivity in the Edwards Aquifer (Halihan, et al., 2000). This scale-dependency is explored further in Section 5. A cross-covariance model was also fitted to model the joint variability between the Y and $\overline{Y}$ variables, which is needed in the cokriging step. The cross covariance (not shown) is well approximated by models of the form of Eq. (3-4), with practical correlation ranges $3\lambda_1$ = 2,700 m and $3\lambda_2$ = 15,000 m.

For the unconfined region, unconditional simulations of K were obtained using the sequential gaussian simulation method as implemented in the SGSIM module of GSLIB (Deutsch and Journel, 1998). The remaining procedure was the same as for the confined region. The upscaling procedure increased the geometric mean K for the unconfined zone by 74 percent

and decreased the log-variance by 29 percent. As with the confined zone, a block-to-point cross covariance model was fitted.

3.3 Cokriging Block Data Based on Local Data

The next step is to estimate the grid-scale conductivity based on the local-scale conductivity measurements. For this step, the log-transformed variables are used. Cokriging provides the best estimate of a spatially distributed variable ($\overline{Y}$ in this case) based on some correlated secondary measurements (Y data from the Mace dataset). The result $\overline{y}_\bullet$ is the best estimate of $\ln \overline{K}$ at each grid block in the management model. The result also provides the kriging variance σ^2_κ, which quantifies the uncertainty in the $\overline{y}_\bullet$ estimate. These two kriging results are shown in Figures 3-5a,b. In constructing these maps, the cokriging estimates for the confined and unconfined zones were merged using maps of the outcrop region provided by USGS. Gray areas are outside the model region. In general, $\overline{y}_\bullet$ is smaller in the unconfined zone as compared to the confined zone because of differences in the underlying Y distributions. The kriging variance is smallest near well locations, but is larger than zero even if the estimation point corresponds to a well location, because the well-scale and block-scale values are imperfectly correlated. The kriging variance is much larger in the unconfined region, indicating large uncertainty in the estimated $\overline{K}$ in the outcrop region. This increased uncertainty is due partly to differences in the Y distribution, but more so to undersampling in the outcrop region.

The final step is to convert the $\overline{y}_\bullet$ to the best estimate of block-scale hydraulic conductivity. Since the kriging system was constructed in terms of the $\overline{Y}$ variable, the resulting kriging result provides $\overline{y}_\bullet$, which is different from the natural log of the best estimate of $\overline{K}$. The two are related through the kriging variance σ^2_K, if one assumes that the posterior distribution is log-normal (e.g., Journel and Huijbregts, 1978).

Best estimates of the $\overline{K}$ field in the Edwards Aquifer are shown in Figure 3-5c. The color scale is on a base-10 logarithmic scale. The largest red regions in the $\overline{k}_\bullet$ map corresponds approximately to the high permeability zone underneath San Antonio, Texas. In general, the expected $\overline{K}$ is slightly smaller in the outcrop region compared with the confined region, but the difference is smaller than for $\overline{y}_\bullet$, as the outcrop region has a larger kriging variance which partially compensates the lower $\overline{y}_\bullet$ in Eq. (3-5).

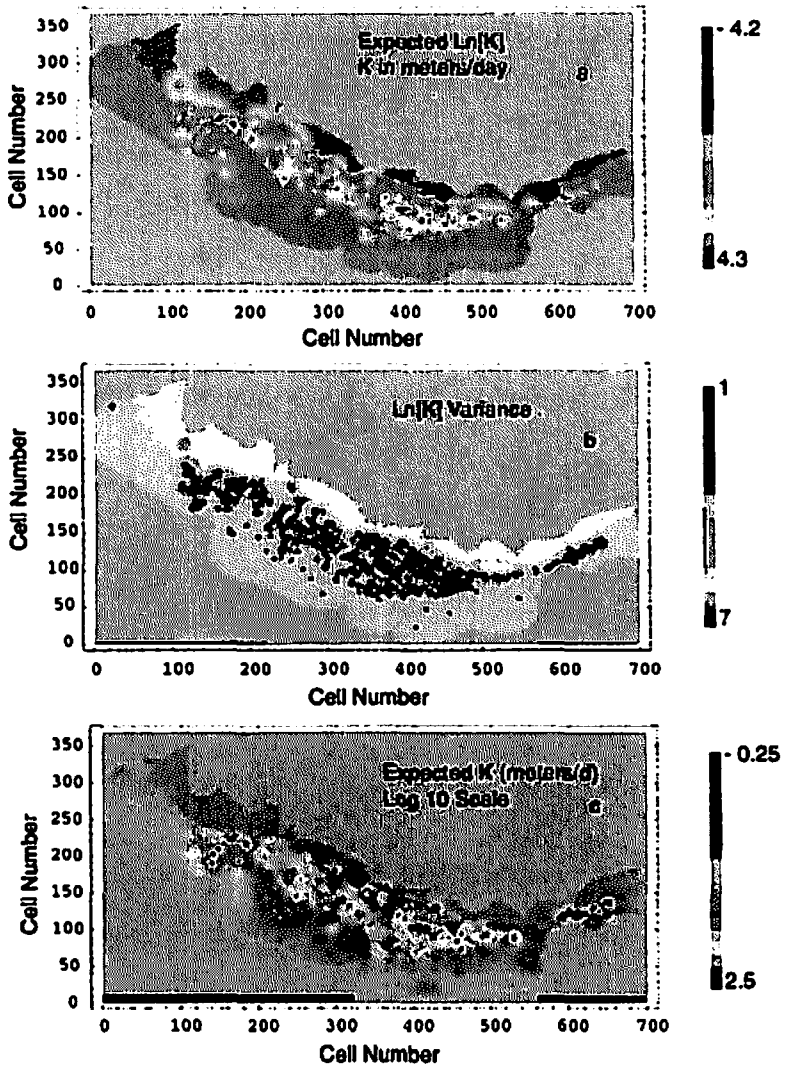

Figure 3-5. Revision 1 of the hydraulic conductivity model for the Edwards Aquifer. Values were obtained by co-kriging block scale quantities conditioned on well scale data. Grid blocks shown in gray are in the inactive regions of the model. The color map in (a) represents best linear unbiased estimate for $\overline{Y} = \ln\overline{K}$ where $\overline{K}$ is block scale hydraulic conductivity in meters/day. The map in (b) shows the kriging variance for $\overline{Y}$. The best estimate for $\overline{K}$ is shown on a base-10 logarithmic scale in (c).

4 REVISION 3: BAYESIAN UPDATING TO MATCH HYDRAULIC HEAD MEASUREMENTS

Revision 1 of the hydraulic conductivity model was based only on well test data and did not utilize the considerable amount of hydraulic head data existing over the Edwards Aquifer region. Hydraulic head data carry considerable information about the underlying hydraulic conductivity distribution. For the same boundary and source conditions, regions of smaller hydraulic gradient imply larger hydraulic conductivity, for example. However, quantitative inference of hydraulic conductivity from hydraulic head data is, in general, difficult. Specifically, this inference requires the solution to an inverse problem, which is nonunique.

Revision 2 of the hydraulic conductivity model is not described here because it is based on a dataset on recharge and hydraulic head that has subsequently been updated by the USGS. In Revision 3 of the hydraulic conductivity model, Revision 1 was taken as a starting point and then modified to be more consistent with measured hydraulic head data. Specifically, a recently developed Bayesian updating procedure (Woodbury and Ulrych, 1998, 2000) was used to update the hydraulic conductivity model. In this approach the nonunique nature of the inverse problem is explicitly acknowledged and the results are given in terms of probability distributions for the hydraulic conductivity in each cell. In addition, the Bayesian method allows prior information of various types to be incorporated into the inversion procedure. This feature allowed the previous work on upscaled hydraulic conductivity to be retained and used in the inversion.

4.1 Bayesian updating procedure

Details of the Bayesian updating procedure are reported elsewhere (Woodbury and Ulrych, 2000). Here we provide a brief qualitative description and discuss some features pertinent to the following discussion. The objective of the inversion is to determine the expected T field of the Edwards Aquifer conditioned on the hydraulic head measurements and the upscaled $\ln(T)$ field. Here T denotes upscaled transmissivity of the aquifer. The solution is not unique because there are fewer equations than unknown model parameters. To obtain a unique solution to the inverse problem, a method for singling out precisely one from the infinite number of solutions is required. In a probabilistic approach we assume that the model is composed of a very large, but finite number of model parameters. The model parameters are assumed to be random and then we approach the inversion from the viewpoint of probability theory. Bayesian solutions can be sought for this problem. The solution is a model that fits the observed data and in some sense minimizes the deviation away from a preconceived notion of behavior of the field.

Before proceeding to the groundwater inversion problem it is useful to review results from Bayesian linear inversion theory. The objective is to find a solution m to a linear inverse problem,

$$d^* = Gm + v \qquad (4\text{-}1)$$

where d^* is an observed data vector, m is the parameter vector to be estimated given d^*, G is a kernel that transforms parameters into data, and v is a noise vector that represents measurement errors. The noise is presumed to have zero mean; that is, the measurements may have some uncertainty, but are unbiased.

In the event that the probability distribution for m and the noise v are multivariate Gaussian, the linear inversion problem has a well known solution (e.g., Tarantola, 1987). Specifically, the distribution of m conditional on d^* is multivariate Gaussian with mean

$$\bar{m} = s + C_p G^T \left(G C_p G^T + C_d\right)^{-1} \left(d^* - Gs\right) \tag{4-2}$$

where C_d is the data covariance, and s and C_p are the mean and covariance for m defined as

$$E(m) = s \tag{4-3}$$

and

$$E\left[(m-s)(m-s)^T\right] = C_p \tag{4-4}$$

The vector s can be thought of as the prior mean for m and the quantity $\bar{m}$ given by Eq. (4-2) is the Bayesian update. The conditional variance can also be determined, but is not addressed here.

Unfortunately, groundwater flow equations in their usual form are not in the required framework for the linear inversion theory. If we associate upscaled transmissivity T with m, then the groundwater flow equations are linear in the parameter as required, but m is not adequately approximated as multivariate Gaussian (e.g., $\ln(T)$ is approximated as multivariate Gaussian, making T lognormal). Conversely, if we associate $\ln(T)$ with m, then m may be adequately approximated as multivariate Gaussian, but then the problem is nonlinear and Eq. (4-2) is not applicable. Woodbury and Ulrych (2000) addressed this issue by employing a perturbation approach to the usual groundwater flow equation. The resulting partial differential equation is linear in $\ln(T)$ and in the form of a (linear) advection-dispersion equation and thus in the form required for application of Eq. (4-2). The advection-dispersion equation can be readily discretized by standard finite-difference or finite-element techniques. The result of this discretization provides the kernel G for use in Eq. (4-2).

It should be recognized that this perturbation approach is strictly applicable only when the variance $\ln(T)$ is less than unity, a condition not met by our upscaled $\ln(T)$ model. However, perturbation approaches often provide acceptable results outside the range of applicability. The

performance of the Woodbury and Ulrych (2000) Bayesian updating procedure has been studied as part of the Master's Thesis of Jiang[1] using synthetic examples with $\ln(T)$ variances as large as 6.8. The root-mean-square error between the hidden "truth" head and the results of the Bayesian update was less than 5 percent of the maximum head difference in the simulation. The findings from these synthetic examples suggest that the Bayesian methodology can be applied to the automatic calibration of two-dimensional steady-state groundwater flow model with large variance of $\ln(T)$.

4.2 Computational Model

The Bayesian updating method requires a conventional groundwater flow model as one step. The existing Bayesian updating code uses a finite-element grid and a corresponding finite-element model of the Edwards Aquifer was constructed. This finite-element model is based on computational grids, pumping data, and boundary conditions provided by the USGS[2] in August 2001, and on recharge data provided by the USGS in January 2002.[3] However, the following simplifications were made in the interest of computational expediency:

- The model is confined throughout the model region as opposed to the USGS groundwater management model of the Edwards Aquifer currently in development, which uses the confined/unconfined mode of MODFLOW. We took the aquifer thickness in the Edwards Aquifer recharge zone to be one-half the aquifer thickness. The effect of this assumption can be removed by using independent information about saturated thickness when converting the updated transmissivity map to hydraulic conductivity.

- Flow from the Trinity Aquifer was neglected. Specifically, the northern boundary of the Edwards Aquifer is modeled as a no-flow boundary. Flow from the Trinity Aquifer is less than 10 percent of the total recharge[4] and this approximation is thus not expected to significantly affect the estimated transmissivity.

- Springs and the Colorado River were made constant head nodes. This is a slightly different condition compared with the drainage and river packages employed in MODFLOW. However, given the large spring conductances for the major springs in the region, the differences between the two approaches are expected to be minor.

To ensure compatibility between the USGS MODFLOW model and the new finite-element model, the finite mesh was designed so that each node is located at the center of an active MODFLOW cell. This mesh was optimally renumbered so that the half-band width of the global

---

[1]Jiang, Y. Personal communication (October 1) to S. Painter, CNWRA. Winnipeg, Manitoba, Canada: University of Manitoba. 2001.

[2]Lindgren, R. Personal communication (August 15) to S. Painter, CNWRA. USGS. 2001.

[3]Lindgren, R. Personal communication (January 15) to S. Painter, CNWRA. USGS. 2002.

[4]Lindgren, R. Personal communication (August 15).

stiffness matrix was limited to as small as 196. The total node number of this finite-element mesh, which is equal to the number of active cells in the MODFLOW grid, is 87,890. Such compatible relation between the two models allows us to transfer data between the two models.

4.3 Calibration Targets

The calibration targets were 153 measurements of steady-state hydraulic head provided by the USGS in August 2001. The location of the head measurements are plotted in Figure 4-1; the color scale represents the hydraulic head value. Of the original 153 measurements, 26 located in regions of extreme gradient of hydraulic head were culled from the target set. These regions of large gradient are situated mostly along the contact between the outcrop and confined zones of the aquifer. They may represent true flow barriers or they may alternatively reflect an error in well location or elevation. Whatever the cause, the large gradient areas caused large numerical error in the inversion method. For that reason those data were removed from the dataset. If the large gradients truly represent flow barriers, then removing those data may cause transmissivity to be over estimated in those regions.

Although the 26 culled data were not used directly in the inversion, they were retained for comparison with the calculated heads as a post-inversion validation exercise (Section 5). Spring flows were treated the same way. Springs were treated as constant-head nodes in the inversion, an approach which offers no direct control over spring discharges. Calculated spring discharges are compared with observed spring discharges in Section 5.

4.4 Prior Model

Revision 1 of the hydraulic properties model was used to set the prior distribution in the inversion process. Specifically, we used maps of the aquifer thickness provided by USGS in conjunction with the expected values of hydraulic conductivity to set the prior $\log(T)$. This prior was modified in the areas immediately surrounding Comal and San Marcos Springs. The borehole data are too sparse to constrain the transmissivity in those areas, and the presence of large-discharge springs suggests that the transmissivity must be large there. The hydraulic conductivity in those areas was set to 6,706 m/d, roughly 1/3 of the largest value in the hydraulic conductivity dataset.

A nested model with integral scales of 1,200 and 5,000 m (practical correlation scales of 3,600 and 15,000 m) and a 50-percent relative nugget effect was used for the spatial covariance, consistent with our geostatistical analyses. The correlation function is written as

$$C_p(k,l) = 0.5\sigma_k\sigma_l\left[\exp\left(-\frac{d}{1200}\right)+\exp\left(-\frac{d}{5000}\right)\right]+0.5\delta(k,l)\sigma_k\sigma_l \qquad (4\text{-}5)$$

where σ is standard deviation of $\ln(T)$, k and l refer to the two nodes in question, d is the distance between two points in meters, and δ is Kronecker number: $\delta = 1$, if $k = l$ and $\delta = 0$ otherwise. For simplicity, this model was assumed to apply across the outcrop and confined zones even though it was developed only for the confined zone. However, the

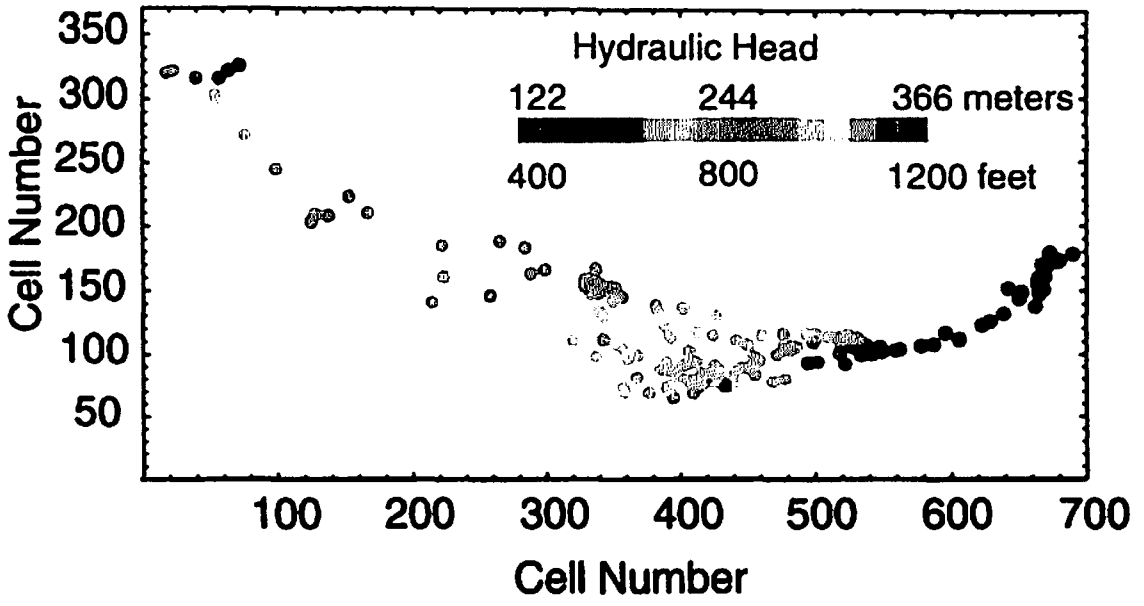

Figure 4-1. Target hydraulic heads used in the Bayesian updating procedure after rotating into the management model grid

variance in the outcrop zone, as calculated in the development of Revision 1, was used unmodified in Eq. (4-1).

4.5 Results

The result of the Bayesian updating procedure, Revision 3 of the hydraulic conductivity model, is provided on the enclosed computer disk. The geostatistical estimates are of vertically averaged hydraulic conductivity instead of transmissivity, consistent with the required input for the confined/unconfined mode of the MODFLOW code. The hydraulic conductivity values are defined on a 700 × 370 grid that is rotated counterclockwise by 35 degrees. The rotation is about the southwest corner located at 428963.81, 3133339.73 in UTM Zone 14 coordinates.

Results are also shown in Figure 4-2. The color scale represents the logarithm of vertically averaged hydraulic conductivity K with warmer colors representing larger K. Locations of major springs and the Knippa Gap are also indicated. In general, the inversion increased K compared with the prior K, especially in the area just east of Knippa Gap.

Calculated heads using the updated K are shown in Figure 4-3. The average error between the calculated and observed heads is 0.15 m, indicating no significant bias in the result. The root-mean-square error and the mean-average-error are 7.0 and 4.6 m, respectively. Given that the difference between the maximum and minimum observed head is about 215 m, this is an excellent agreement. When the 26 culled heads are returned to the target set, the agreement is still good, as will be discussed in Section 5.

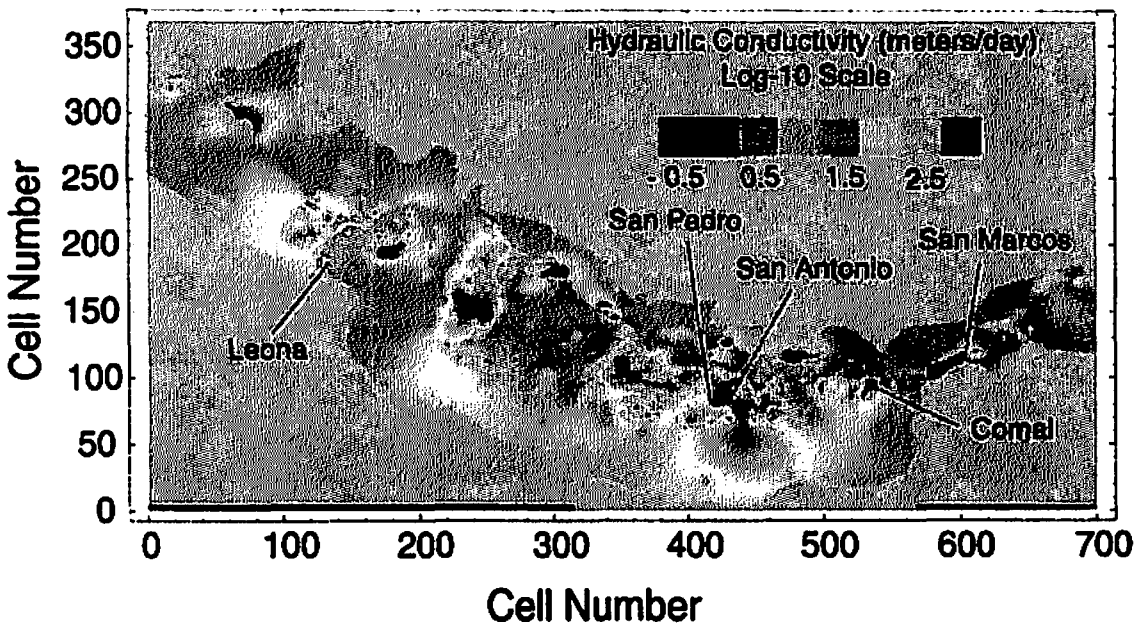

Figure 4-2. Revision 3 of the hydraulic conductivity model of the Edwards Aquifer obtained by Bayesian updating

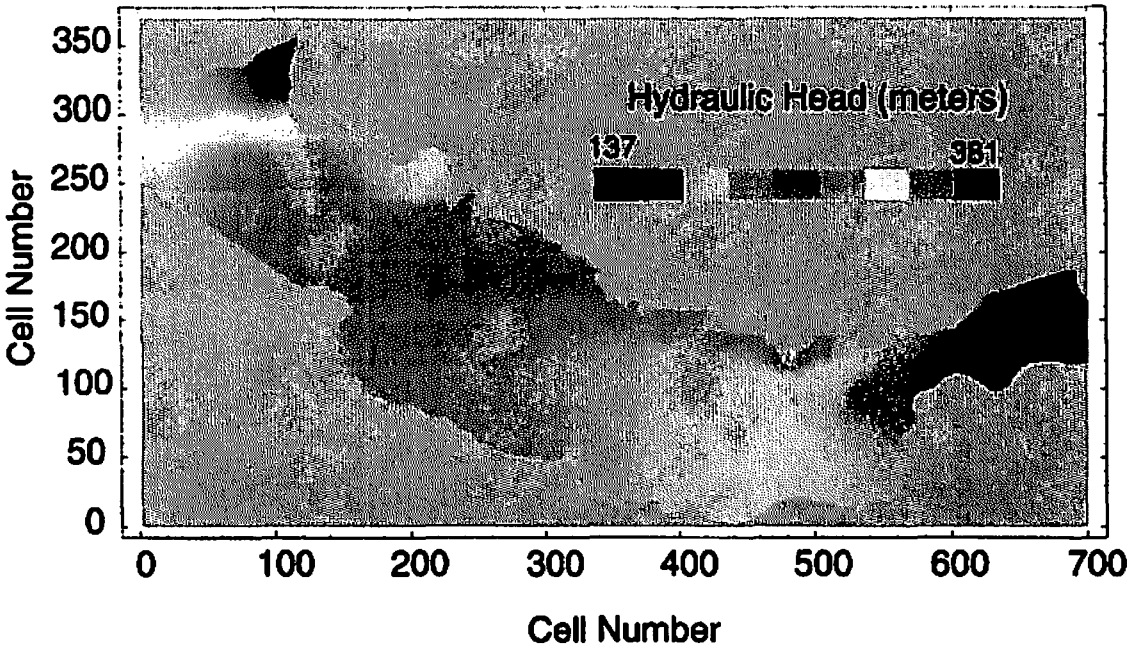

Figure 4-3. Calculated hydraulic heads resulting from Revision 3 of the hydraulic conductivity model

5 PERFORMANCE OF THE HYDRAULIC CONDUCTIVITY MODELS

The performance of the hydraulic conductivity models is evaluated in this section. Specifically, Revisions 1 and 3 of the hydraulic conductivity model are input into the finite-element model described in Section 4, and the success at matching observed hydraulic heads and spring flows is evaluated. For comparison purposes, a simple hydraulic conductivity model created by kriging without upscaling is also included. In addition, the results are compared with empirical trends relating average hydraulic conductivity to scale of investigation. This section is intended to quantify the improvement obtained in the hydraulic conductivity model over a basic spatial interpolation of the Mace (2001) dataset.

5.1 Scale Dependence

One of the key goals of this project was to address the dependence of hydraulic conductivity on spatial scale of investigation. It has been noted previously (Halihan, et al., 2000) that effective hydraulic conductivity in the Edwards Aquifer tends to increase with spatial scale of support. Specifically, the geometric means from core measurements, single well tests, and calibrated groundwater models as compiled by Mace (2001) form a nearly straight line when plotted against spatial scale on a double logarithmic plot. Neglecting this scale dependence would have introduced significant bias in the resulting hydraulic conductivity map. The geometric means of Revisions 1 and 3 of the hydraulic conductivity model are shown on the same type plot in Figure 5-1. The upscaling procedure underlying Revision 1 increased the geometric mean hydraulic conductivity by 67 percent over that of the Mace (2001) dataset, as the spatial scale is increased by a factor of 20. This increase with increasing scale is consistent with the previously identified trend, but is below the trend line. The Bayesian updating procedure increases the geometric mean to about 46 m/d, which corresponds to a factor of 7 increase over that of the Mace dataset. This value of 46 m/d for the geometric mean is close to the previously identified trend line, which provides confidence in the result of this study. It is emphasized that this increase was accomplished without resorting to ad-hoc adjustment of the hydraulic conductivity distribution.

5.2 Match to Hydraulic Heads and Spring Flows

Revisions 1 and 3 were input into the finite-element groundwater flow model described in Section 4, and the resulting hydraulic heads and spring flow rates were compared with observed values. A hydraulic conductivity model created by spatially interpolating (kriging) the Mace (2001) dataset with no upscaling was also input into the groundwater flow model, for comparison purposes. The target hydraulic head dataset included 153 measurements (i.e., the 26 that were removed for the Bayesian inversion are reintroduced in this validation exercise). Springs were modeled by fixing the hydraulic head at the spring locations and calculating the discharges. The hydraulic head in the vicinity of San Antonio Springs is lower than the spring elevation in all the models; therefore, discharges from this spring were ignored (i.e., the spring is dry in the simulations).

Calculated versus observed heads are plotted in Figure 5-2. Quantitative measures of the agreement between the calculated and observed heads are provided in Table 5-1. The improvement obtained in this work can be seen by comparing Figure 5-2a with Figure 5-2c. The hydraulic conductivity model obtained by kriging produces significant error in the predicted

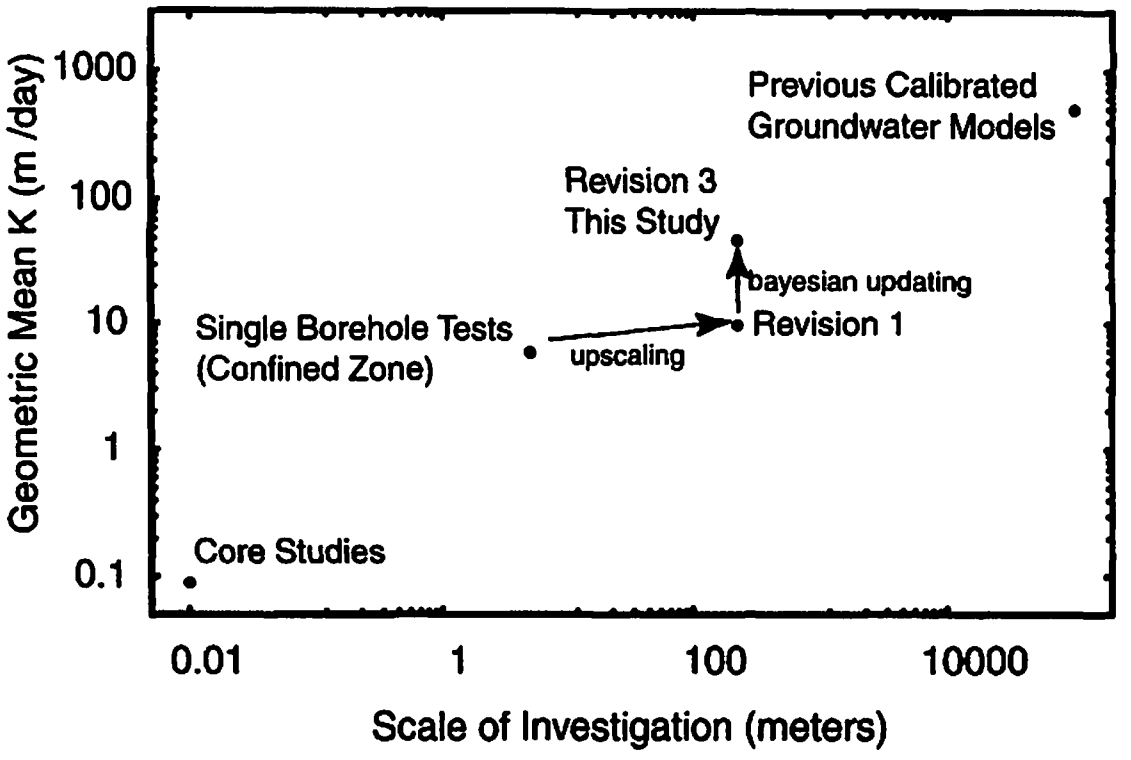

Figure 5-1. Geometric mean hydraulic conductivity (meters/day) versus scale of support for the Edwards Aquifer. The geometric mean generally increases with increasing scale of support (averaging volume) because of multiple-scale heterogeneity. The geometric mean of the upscaled hydraulic conductivity obtained in this study through numerical simulation is consistent with the general trend. The other geometric means are as compiled by Mace (2001).

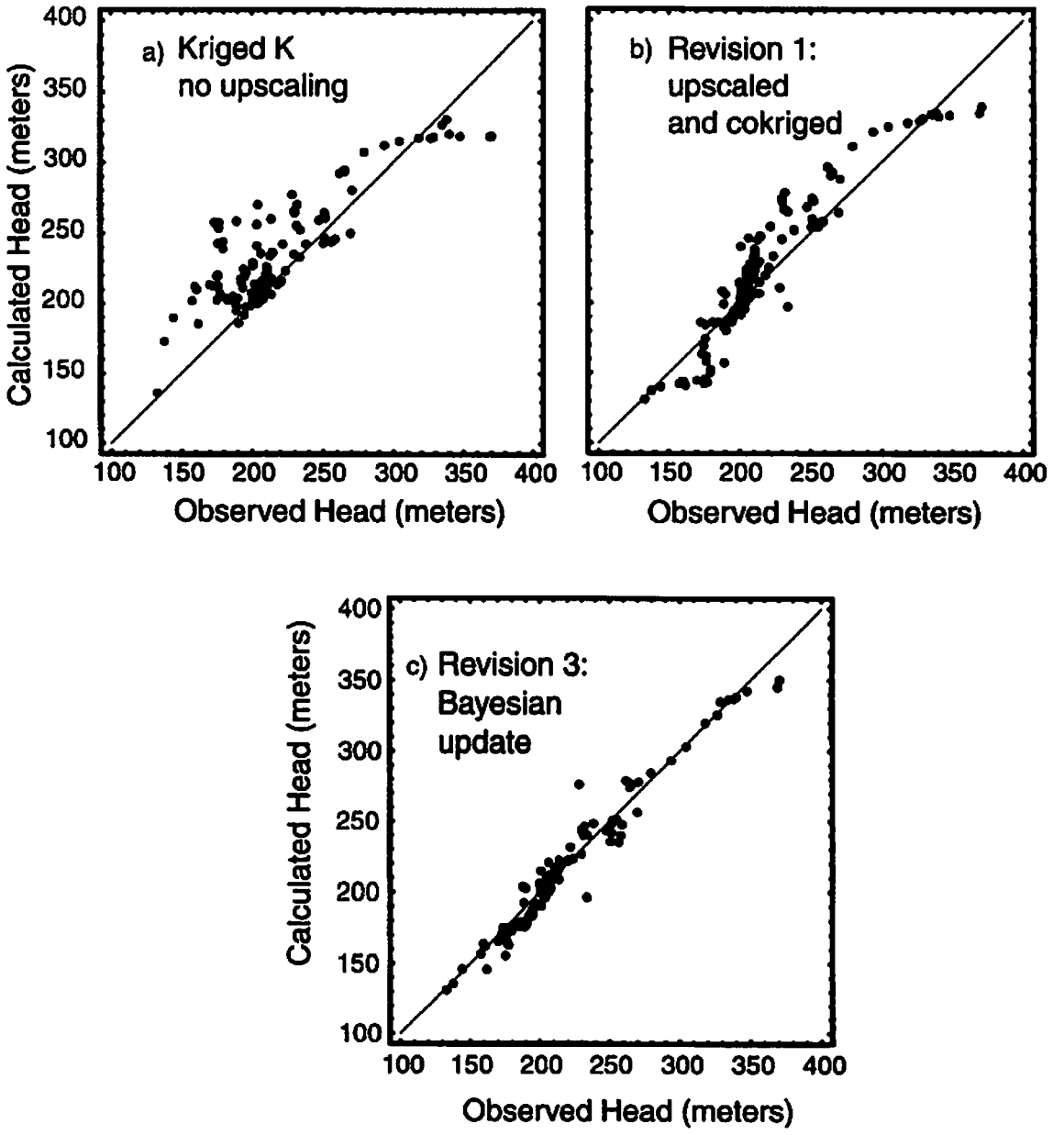

Figure 5-2. Cross plot of observed and calculated heads showing successive improvement with each hydraulic conductivity refinement

Table 5-1. Improvements in hydraulic head error obtained in this project. The total head drop across the region is about 250 meters. Values are in meters.			
	Kriged K, No upscaling	Revision 1, Upscaled/Cokriged	Revision 3, Bayesian Update
Mean error	- 12.9	- 3.9	1.2
Root-mean-square error	26.1	17.2	8.2
Mean-absolute-error	17.5	12.5	6.0
Maximum error	84.2	45.9	48

hydraulic heads. In particular, there is a large spread and a significant bias in the heads produced by the kriged model. These errors are reduced greatly in Revision 3; the mean error is reduced by more than a factor of 10, and the mean absolute error is reduced by a factor of 3. For Revision 3, the mean absolute error is 6 m, which is roughly 2.5 percent of the total head drop across the Edwards region, representing excellent agreement. This excellent agreement between calculated and observed heads clearly demonstrates the utility of the automatic calibration techniques applied in this work.

Obtaining a groundwater model fully calibrated to spring flows in not within the scope of the present project. Such a calibration will be accomplished by the USGS once the model inputs on recharge, pumping and boundary conditions are finalized. Therefore, no significant attempt was made to match spring flows. Nevertheless, Revision 3 of the hydraulic conductivity model still produced significant improvements in the spring flows as compared with the kriged model (Table 5-2). Specifically, the spring discharges in the down-gradient regions are roughly consistent with the calibration set, with the main exception being San Antonio Spring, which is dry in the simulations. Flow at Leona Spring is also significantly larger than the calibration value of 0.425 m^3/s. However, this discharge rate does not account for the potentially large losses into the highly permeable Leona Gravel formation. For this reason, no attempt was made to match discharge at Leona Spring.

Table 5-2. Improvements in calculated spring flow obtained in this project. Values are spring discharges in cubic meters per second.				
	Kriged K, No Upscaling	Revision 1, Upscaled/Cokriged	Revision 3, Bayesian Update	Calibration Target
San Marcos	0.584	0.478	2.24	4.22
Comal	6.91	6.55	7.62	9.34
San Antonio	0*	0*	0*	0.283
San Pedro	6.24	3.68	0.325	0.181
Leona	4.06	3.40	4.76	0.425†

*Hydraulic head at node corresponding to spring is less than spring elevation. Spring is not flowing.
†Does not include losses into Leona Gravel Formation. May be significantly less than true discharge from Edwards Aquifer. No attempt was made to match this value.

6 PROPOSED APPROACH FOR REFINING THE HYDRAULIC CONDUCTIVITY MODEL

One of the main products of this work is the development of a general quantitative framework that makes it possible to combine various types of data. We used a Bayesian approach to combine data on aquifer thickness, boundary conditions, recharge, pumping rates, spring discharge rates, observed hydraulic heads, and well-derived transmissivities in a self-consistent manner that honors the physics of groundwater flow. The Bayesian methodology also has the flexibility to incorporate some types of geological information. In this section, we outline approaches that could be used to further refine the hydraulic conductivity model.

The first suggested refinement is to incorporate the latest data on boundary conditions and recharge from the evolving USGS effort. The final properties model utilizes a preliminary dataset on recharge that has subsequently been refined by the USGS. To expedite the model development, inflow from the Trinity aquifer was also neglected and a crude approximation was used for the saturated thickness in the outcrop zone. Now that the computer codes are in place to accomplish the Bayesian inversion, these refinements could be made with modest additional effort.

The second suggested refinement is to employ a finer computational grid in regions of large hydraulic gradient. As was noted in Section 5, the approximations underlying the Bayesion methodology break down when the hydraulic gradients become large. Large hydraulic gradients can occur near pumping wells and in regions of low hydraulic conductivity. It was found empirically that good results are produced if the head difference between two adjacent computational cells is sufficiently small. This condition is not met over all regions of the model grid, but acceptable results could still be achieved by simply removing hydraulic head data associated with very high gradients. This data culling has the effect of spreading in space what would otherwise be narrow flow barriers. When viewed at sufficiently large scales, the resulting smearing of the low hydraulic conductivity features does not appear to significantly affect the flow. However, it does introduce potential errors in the calculated water levels near the features. This inaccuracy in regions of high gradient is not a fundamental limitation and could be eliminated by simply refining the computational grid. Specific areas that could benefit from grid include the areas around Comal and San Marcos Springs, and the contact between outcrop and confined regions.

An additional refinement could be made by incorporating geological information on the location of potential conduits. This information is straightforward to include within the Bayesian framework by modifying the prior distribution. The prior distribution represents the best guess at the hydraulic conductivity map prior to enforcing the constraints on hydraulic heads, and could include expert judgment on the location of high or low permeability zones as one component. Indeed, we took a preliminary step down this path by enhancing the prior hydraulic conductivity in the areas around Comal and San Marcos Springs. The specific approach would be to add zones of enhanced conductivity corresponding to mapped conduits. Uncertainty in the position of these conduits would be included by assigning a finite width to the high conductivity zones. The Bayesian updating procedure would then adjust the values of hydraulic conductivity in these zones to be consistent with the measured hydraulic heads.

7 CONCLUSIONS

The successive improvements in the performance of each refinement of the hydraulic conductivity model, as demonstrated in Section 5, clearly show the utility of adopting a formal statistical approach to parameter estimation. Such an approach minimizes subjective input and manual adjustment of the hydraulic conductivity model, thereby maximizing defensibility against external challenges.

A fully calibrated model was not one of the original goals of the project, and will be addressed using conventional hand calibration by USGS staff. Nevertheless, a partially calibrated model was achieved, which provides an excellent starting point for transient calibration. In addition, with additional refinements outlined in Section 6, the approach could be used to do fully automatic calibration, at least in steady state.

These results also provide some insights into the relative value of different types of data. Specifically, the improved performance of the hydraulic conductivity model in going from Revision 1 to Revision 3 underscores the degree to which hydraulic head measurements carry information about the underlying areal distribution of hydraulic conductivity. Additional efforts to improve and expand the database of water level measurements, through compilation of existing data and ongoing water level monitoring, may be the most cost-effective approach to improving the hydraulic conductivity model. This approach requires solution of an inverse problem, similar to what was achieved here, and would therefore benefit from the refinements suggested in Section 6.

The specific approach adopted, a Bayesian updating procedure, has some powerful features that were not fully exploited in this project. Specifically, it provides a framework for merging direct measurements of hydraulic heads and hydraulic conductivity with semi-quantitative information in the form of expert judgment from geologists. This fusion of direct measurements with expert geological judgment is a largely unexploited approach that could greatly improve future revisions to the hydraulic conductivity model.

8 REFERENCES

Deutsch, C.V. and A.G. Journel. *Geostatistical Software Library and User's Guide*. 2nd Edition. New York City, New York: Oxford University Press. 1998.

Halihan, T., R.E. Mace, and J.M. Sharp. "Flow in the San Antonio Segment of the Edwards Aquifer: Matrix, Fractures, or Conduits?" *Groundwater Flow and Contaminant Transport in Carbonate Aquifers*. I.D. Sasowsky and C.M. Wicks, eds. Rotterdam, Netherlands: A.A. Balkema Publishers. 2000.

Hovorka, S.D., R.E. Mace, and E.W. Collins. *Permeability Structure of the Edwards Aquifer, South Texas-Implications for Aquifer Management*. Bureau of Economic Geology. The University of Texas at Austin. Report of Investigations No. 250. Austin, Texas: The University of Texas. 1998.

Journel, A.G. and Ch.J. Huijbregts. *Mining Geostatistics*. San Diego, California: Academic Press Limited. 1978.

Mace, R.E. "Determination of Transmissivity from Specific Capacity Tests in a Karst Aquifer." *Ground Water*. Vol. 35, No. 5. pp. 738–742. 2000.

Mace, R.E. and S.E. Hovorka. "Estimating Porosity and Permeability in a Karstic Aquifer Using Core Plugs, Well Tests, and Outcrop Measurements." *Groundwater Flow and Contaminant Transport in Carbonate Aquifers*. I.D. Sasowsky and C.M. Wicks, eds. Rotterdam, Netherlands: A.A. Balkema Publishers. 2000.

Tarantola, A. *Inverse Problem Theory (Methods for Data Fitting and Model Parameter Estimation)*. New York City, New York: Elsevier. 1987.

Woodbury, A.D. and T. J. Ulrych. "A Full-Bayesian Approach to the Groundwater Inverse Problem for Steady State Flow. *Water Resources Research*. Vol. 36, No. 8. pp. 2,081–2,093. 2000.

Woodbury, A.D. and T.J. Ulrych. "Minimum Relative Entropy and Probabilistic Inversion in Groundwater Hydrology. *Stochastic Hydrology and Hydraulics*. Vol. 12. pp. 317–358. 1998.